Original Article

Experimental analysis of impact and post-impact behaviour of inserts in Carbon sandwich structures

Laurent Mezeix[1], Simon Dols[2], Christophe Bouvet[2], Bruno Castanié[2], Jean-Paul Giavarini[3] and Natthawat Hongkarnjanakul[4]

Abstract

In aeronautics, honeycomb sandwich structures are widely used for secondary structures such as landing gear doors, flaps or floors, and for primary structures in helicopters or business jets. These structures are generally joined by using local reinforcements of the insert type. In the present study, 50 J low velocity impact tests were performed on inserts using a drop-weight device and the impact response and failure patterns were analysed. Impacted specimens were then pull-through tested to failure. Some of the tests were stopped before final failure in order to obtain precise details on the failure scenario. It was shown that, in the cases studied, the residual strength after impact was very high (about 90%) in comparison to the large reductions habitually observed in compression after impact tests.

[1]Faculty of Engineering, Burapha University, Chonburi, Thailand
[2]Université de Toulouse; ICA (Institut Clément Ader); INSA, ISAE, UPS, Mines Albi, UMR CNRS 5312, Toulouse, France
[3]Sogeclair Aerospace, Blagnac, France
[4]Geo-Informatics and Space Technology Development Agency, Space Krenovation Park (SKP), Chonburi, Thailand

Corresponding author:
Bruno Castanié, Université de Toulouse; ICA (Institut Clément Ader); INSA, ISAE, UPS, Mines Albi, UMR CNRS 5312, 3 rue Caroline Aigle, 31400 Toulouse, France.
Email: bruno.castanie@insa-toulouse.fr

Keywords
Carbon Laminates, impact, insert, pull-through, sandwich

Introduction

Inserts in sandwich structures are widely used in many fields, such as aeronautics, space and marine or civil engineering. The literature contains a very large number of studies concerning impacts on sandwich structures and their strength after impact (e.g. see literature [1–5]). Sizing methodologies for impact have also been proposed [6] and then evaluated [7] but the specific problem of impact on junctions has not been addressed. Neither is this issue treated in reference books on impact in sandwich structures [8, 9]. In general, studies on inserts focus on static sizing methods based on analytical models that are more or less relevant; details can be found in the literature [10–12]. These methods are effective in practice as long as appropriate allowables are taken. Thomsen et al. [13–15] have developed refined analytical models that represent the stress concentrations well at the skin/insert/core triple point and propose design rules for fully potted or partially potted inserts. An interesting application of these theories is found in the horizontal gradients of foam core that have been proposed to reduce stress concentration [16]. Nevertheless, these methods are limited to the linear domain. Bunyawanichakul et al. [17,18] have shown that the failure scenario of a fully potted insert under pull-through is complex: core shear buckling and tears in the vicinity of the insert, crushing of the potted insert under the screw head and then punching of the laminate skin. These authors propose a nonlinear finite element model to capture this scenario. Other research efforts have focused on various themes such as the strength variability of an insert in relation with the manufacturing process [19], the reliability of inserts [20], the development of new technologies [21], the development of automated methods of installation [22] and the behaviour of inserts under environmental effects [23]. Enhanced FE Software and finite element formulation have allowed some authors to propose very refined models. Heimbs and Pein [24] have partially modelled insert tearing by representing the honeycomb core with its actual geometry and capturing the buckling of the cells in the vicinity of the insert. Roy et al. [25] used a similar strategy to model the pull-through of metallic inserts. Their proposed model simulates the linear load/displacement portion of the insert pull-out properly and closely predicts the onset of stiffness reduction. An experimental study was conducted by Song et al. [26] to investigate the effect of design variables, such as the core height and density, the face thickness and the insert clearance, on the failure loads of a sandwich insert joint. However, despite the obvious interest of the topic, the authors have found no papers on the subject of impact and insert (except their own conference papers [27,28]) and the subject is worthy of investigation.

So, the aim of this paper is first to analyse the damage due to an impact on an insert. There is a wide range of inserts and the choice made here was to use the

same technology as Bunyawanichakul et al. [17,18]. Impact tests were a priori performed on the insert and some distance away from it. The failure patterns were analysed. Then pull-through tests were conducted in the same way as in Bunyawanichakul et al. [17,18] or Adam et al. [29]. Stopped tests were also used in order to propose a failure scenario. Finally, some conclusions on modelling strategies are proposed.

Materials and methods

The core was made of Nomex^{TM} honeycomb with a cell size of 4.8 mm, a density of 48 kg/m^3 and a thickness of 10 mm. The potted inserts were made with 3 M Scotch-Weld^{TM} 3500-2B/A. The Nomex cells were filled with an in-house tool as shown in Figure 1. The diameter of the insert was about 30 mm. The shape obtained was almost the same as in Raghu and Battley [19] and dispersion could not be avoided. The insert was cured at 175°C for 1 h. The skins were manufactured and cured separately. They were made of unidirectional carbon ply impregnated with dry resin and a hardener mixture (Araldite LY 5052 and hardener HY 5052) baked for 4 h at 80°C under a pressure of 7 bar. Two different skins were made: a thick skin (lower skin $[45, 90, -45, 0]_{2s}$, 3.2 mm thick) and a thinner skin (top skin $[45, 90, -45.0]_s$, 1.6 mm thick). This choice was related to an innovative aeronautic floor designed by the industrial partners. The core and the skins were bonded with a redux film under vacuum at 120°C for 1 h to form $140 \times 140\,mm^2$ sandwiches after trimming. Finally, a hole of diameter 6.35 mm was drilled in the centre of each test piece (Figure 2). Fourteen specimens were manufactured (12 for impact tests and two pristine).

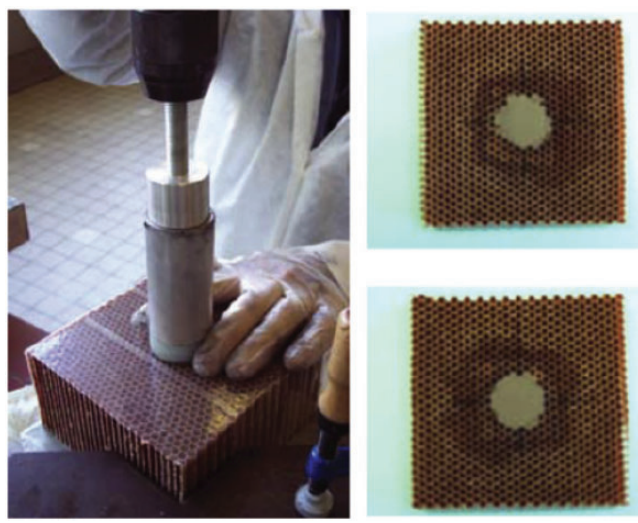

Figure 1. Manufacturing of the potted insert.

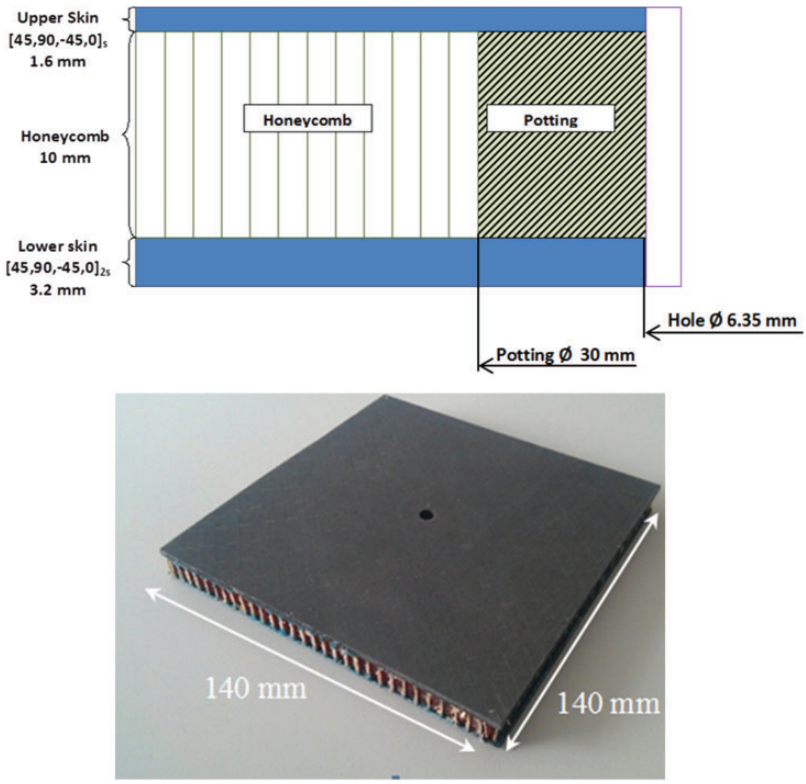

Figure 2. Design and photo of finished sample.

Impact tests were performed using a drop tower system (same as in Castanié et al. [1]) with a 4 kg spherical impactor 16 mm in diameter. They followed the Airbus Industries Test Method (AITM 1-0010) (Figure 3(a)), except for the size of the specimen ($140 \times 140\,mm^2$) which was different because of the post-impact tests. The square specimens simply sat on a $120 \times 120\,mm^2$ frame. The velocity of the impactor was measured with an optical laser just before its impact with the specimen. A piezoelectric force sensor was placed inside the impactor to measure the acceleration during contact, which allowed the contact force during impact to be computed. The displacements of the rear face were measured by a second laser sensor. The anti-rebound system was manual, economic and efficient; it comprised a simple plank of wood driven by a quick young human neuronal system (Figure 3(b)). The specimen was then positioned so that, a priori, impact occurred on the insert or the honeycomb alone. Several tests at different impact energies were performed and an energy of 50 J was selected so that a residual dent >0.3 mm Barely Visible Impact damage (BVID) remained visible.

The same device as used by Bunyawanichakul et al. [17,18] was employed to perform pull-through tests with a 100 kN Instron testing machine (Figure 4).

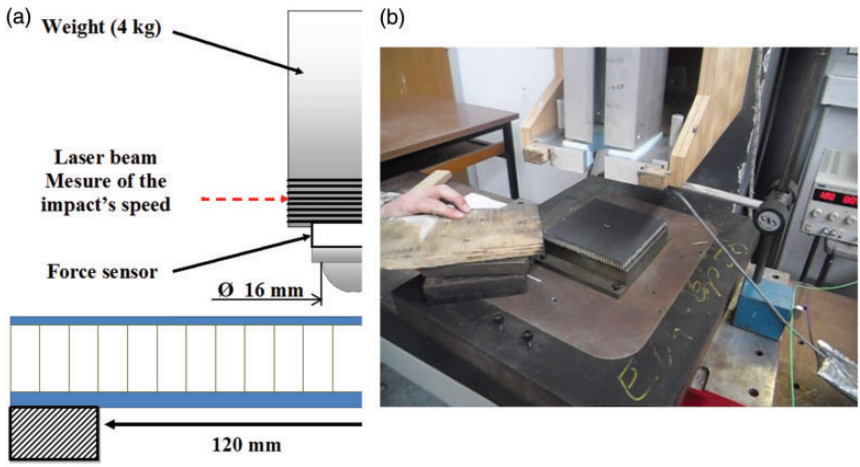

Figure 3. Impact device (a) details and (b) overview.

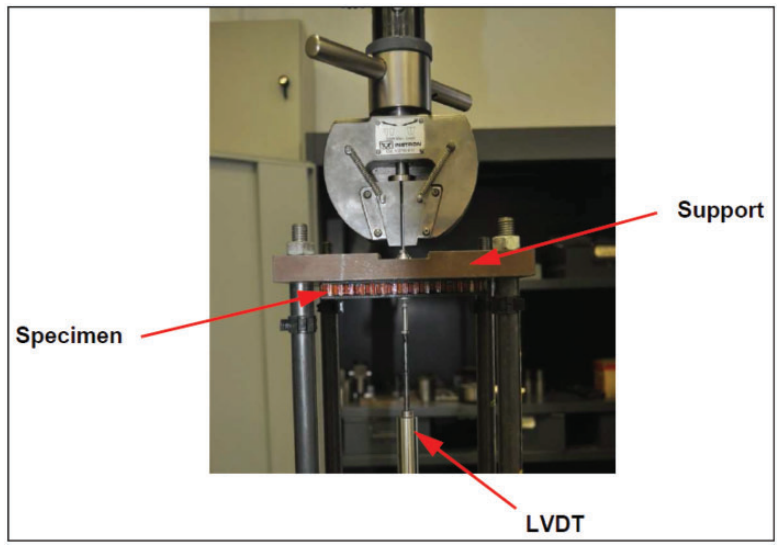

Figure 4. Overview of pull-through tests.

The specimen was simply supported on a square frame with an internal window of $110 \times 110\,mm^2$. A machined bolt (NAS 6704-91) was mounted on the specimen as shown in Figures 5 and 6. Then the nut was hand tightened and thus the insert was held between the bolt head and the spacer. The grips of the traction machine were applied to the machined part of the screw. A displacement sensor measured the displacement of the screw head during the test and the tensile force was given by the load cell of the machine. The test consisted of pulling the screw until it punched

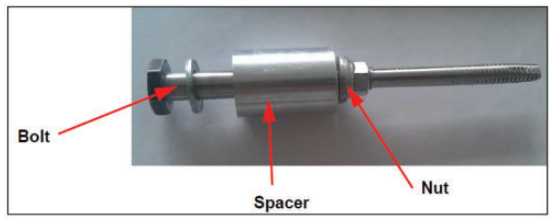

Figure 5. Machined bolt for loading the insert.

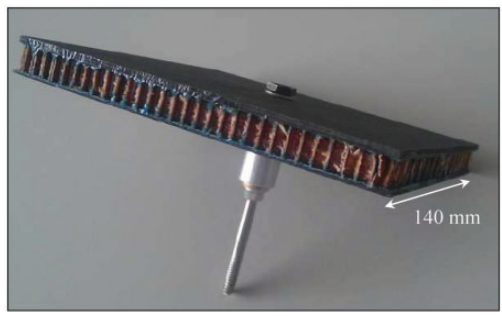

Figure 6. Specimen ready for pull-through tests.

through the lower skin, leading to collapse of the structure. The test was displacement controlled at a speed of 2 mm/min.

Analysis of impact tests

Discussion on impact location

Tests showed that there were three impact positions that generated quite different responses and damage scenarios: on the insert (case 1, Figure 7), on the border of the insert (case 2, Figure 7) and on the core (case 3, Figure 7). The geometric dispersion due to the traditional method of filling cells increased the experimental dispersion of this phenomenon, as already reported by Raghu and Battley [19]. The force/displacement curves were actually quite different (Figure 7) but the dispersion between the impact locations was low, allowing the impact site to be found a posteriori and the cases to be ranked. The peak force was higher in the case of an impact on the insert, which was to be expected given the greater stiffness of the structure. Moreover, all curves had the same, globally sinusoidal, beginning corresponding to a linear response of the structure, followed by clear force drops indicating that the cells of the honeycomb were first damaged by shear buckling of the cell edges in the vicinity of the potted insert [1,2,9]. This is consistent with what has already been reported in the literature. On the other hand, a very significant difference was observed between the impacts on the insert and on the core

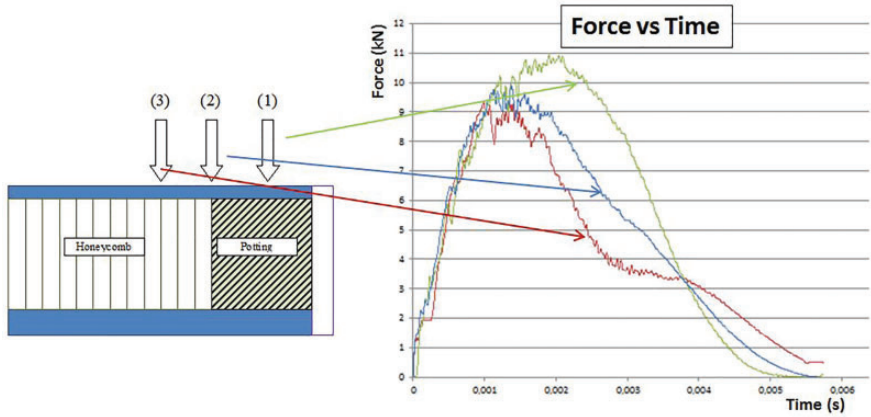

Figure 7. Influence of impact location on the impact response of the insert.

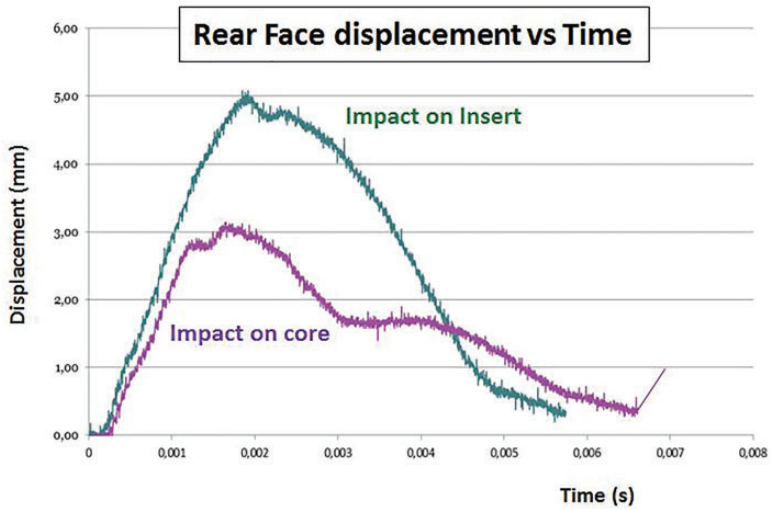

Figure 8. Rear face displacement versus time for impact on the insert and on the core.

(Figure 8) for the displacements of the rear face, indicating that a very different failure scenario occurred. It was also noted that the peak force was about 20% higher when the impact was on the insert.

Damage analysis for impact on the insert (case 1)

The tests were sorted and collected by impact position category. For three impact tests on the insert, the force/displacement curves are shown in Figure 9.

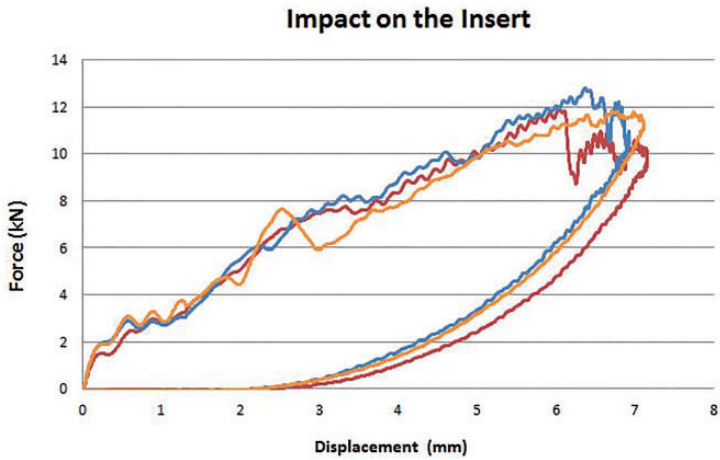

Figure 9. Force/displacement responses for impact on the insert.

The dispersion is low, which shows that the failure scenario is probably still the same for a given configuration. The shape of these curves is very similar to those observed for impact on laminate [30], suggesting that the honeycomb plays only a small role. To confirm this analysis, C-scans were carried out and vertical sections were cut (Figures 10 to 12). It appears that the indentation was very small (Figure 10(a)) when the impact was on the insert. This is why the relatively high impact energy of 50 J was used. The damage in the upper skin was located to the right of the impactor. Some damage appeared in the honeycomb but was limited to two or three circumferential cells around the insert. The skin was crushed locally at the impact but the damage was contained. Under the impact location, the insert seemed intact but the lower skin had significant damage. The C-scan (Figure 11) showed very large delaminations oriented on the side of the impact location. These were also visible in the micrographic section (Figure 12). It seems, therefore, that the insert retransmitted most of the energy of the impact to the lower skin. This confirms (i) that the predominant damage occurred in the lower laminated skin and (ii) the a priori analysis of the shape of the force/displacement curve.

Damage analysis for impact on the border of the insert (case 2)

The load/displacement curves for three samples are given in Figure 13. Qualitatively, the shape of the curve is quite different with a fairly large plateau that is typical of the response of honeycomb core sandwich to impact [1–9]. There is no peak force but the plateau force is about 20% less than the maximum force for an impact on the insert. The same type of analysis was conducted with post-mortem microscopic observation and C-scans (Figures 14 and 15). The residual indentation was more marked, with the appearance of broken fibres on the surface of the upper skin. Damage was also different in the core and in the insert. The insert

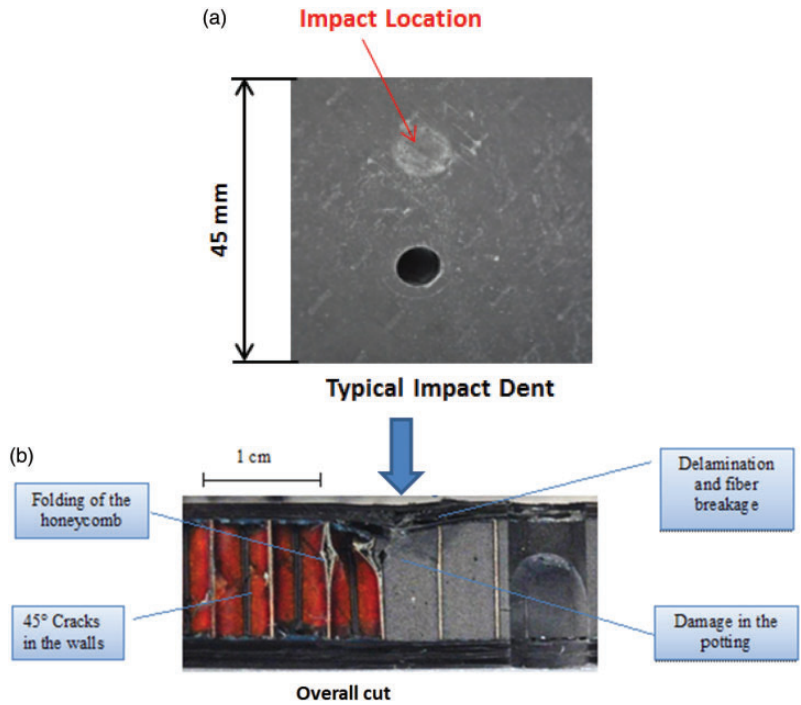

Figure 10. (a) Typical dent after impact on the insert and (b) post-mortem observation of a specimen.

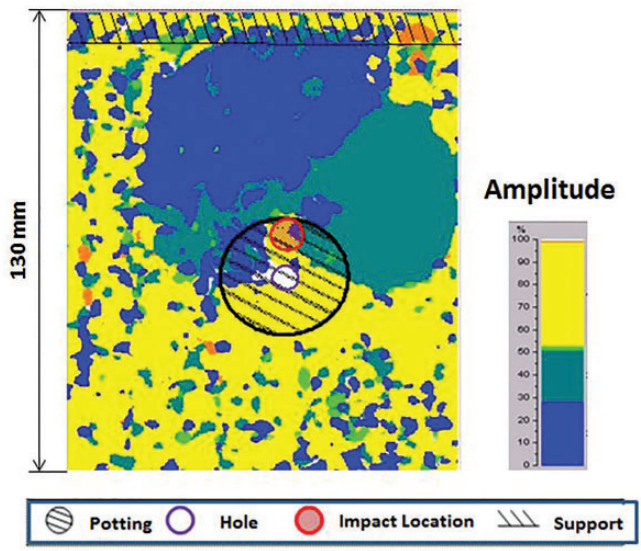

Figure 11. C-scan of the lower skin after an impact on the potted insert.

Figure 12. Micrographic section of lower skin after an impact on the potted insert.

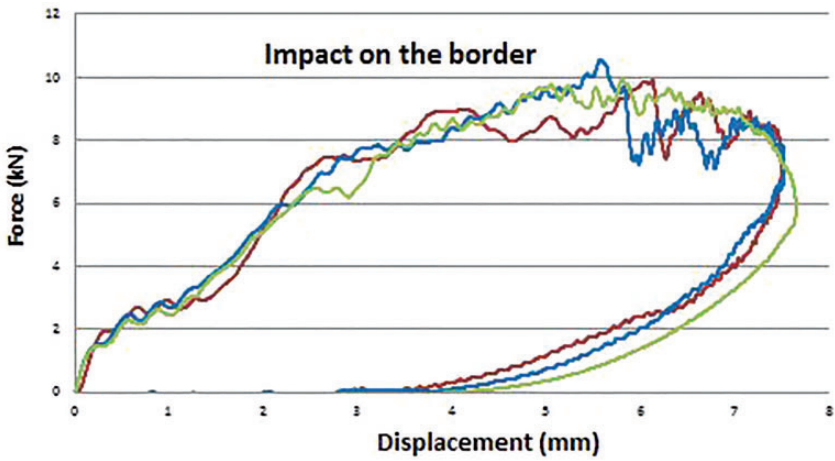

Figure 13. Force/displacement responses for impact on the border of the insert.

was crushed on half its thickness and the honeycomb core was also crushed locally [31]. A C-scan of the lower skin showed large delaminations similar to that observed in the case of a direct impact on the insert. So in this case, even though the insert was observed to have undergone localized crushing, it remained sufficiently rigid during an impact to transmit the forces to the lower skin and to create large delamination. There was also marked damage to the upper skin (fibre breakage) but it remained localized around the impact. Qualitatively, the energy dissipated (area inside the force/displacement curve) was greater in this case than in the other two configurations, probably because the effects of several damage modes were accumulated.

Damage analysis for impact on the core (case 3)

The load/displacement curves for three samples are given in Figure 16. Here, we find the classic response of sandwich structures with Nomex honeycomb core under impact [1–10]. In this case, the plateau area is smaller than in the previous case

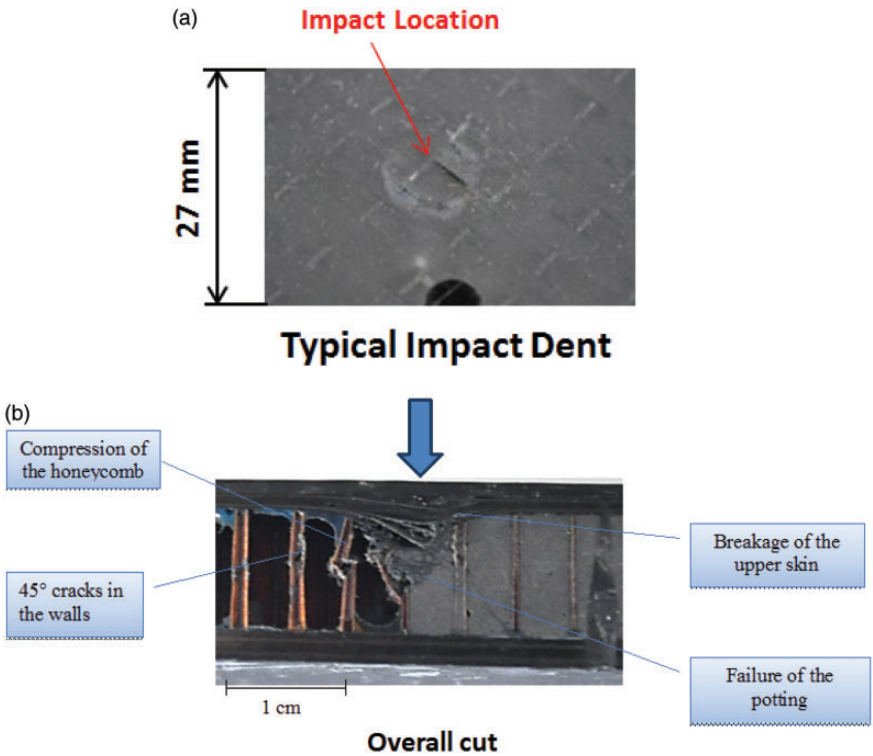

Figure 14. (a) Typical dent after impact on the border of the insert and (b) post-mortem observation of a specimen.

because there is energy absorption in the core, which explains the decrease of force at the end of the test and the absence of rebound. Because of the high impact energy (50 J), the upper skin was perforated (Figure 17) and the honeycomb significantly crushed [31]. However, as shown in the C-scan of Figure 18, no delamination damage was apparent in the lower skin, which confirms the force transmission role of the insert during the impact and the absorption role of Nomex honeycomb which protects the lower skin.

Summary

A summary of the damage in the three cases is proposed in Table 1. The damage patterns differ significantly from one case to another. Especially when the impact occurs on the insert or even on its edge, the stiffness is sufficient to transfer impact force to the lower skin. So large delamination occurs in this lower skin although only a small part of the upper skin is damaged at the right of the impact. The delamination patterns are original and only one side of the specimen is affected, the rest being somehow ‘‘protected’’ by the insert. This is very different when

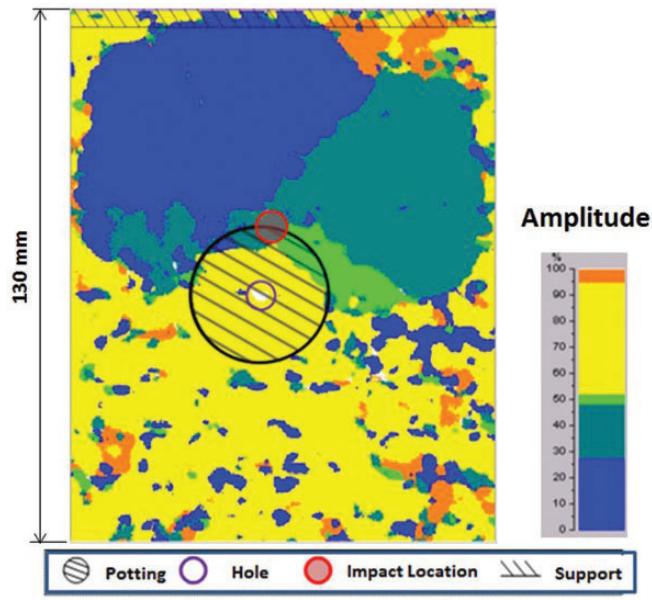

Figure 15. C-scan of the lower skin after an impact on the border of the insert.

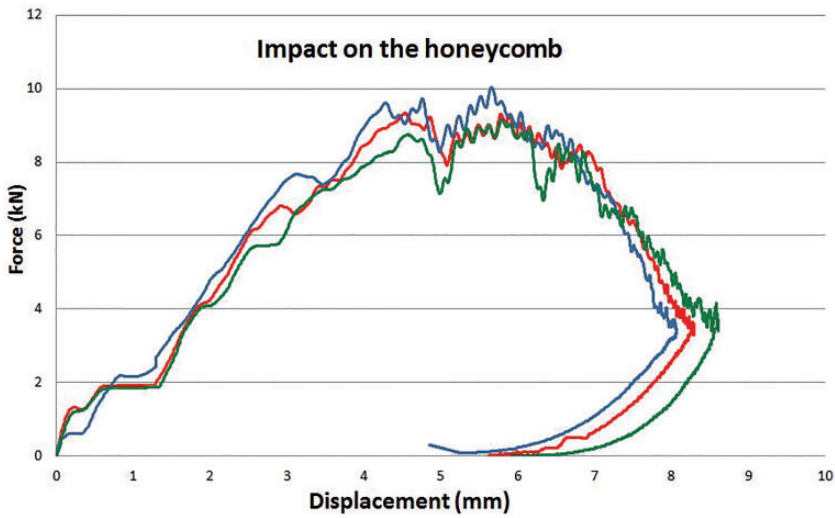

Figure 16. Force/displacement responses for impact on the honeycomb core.

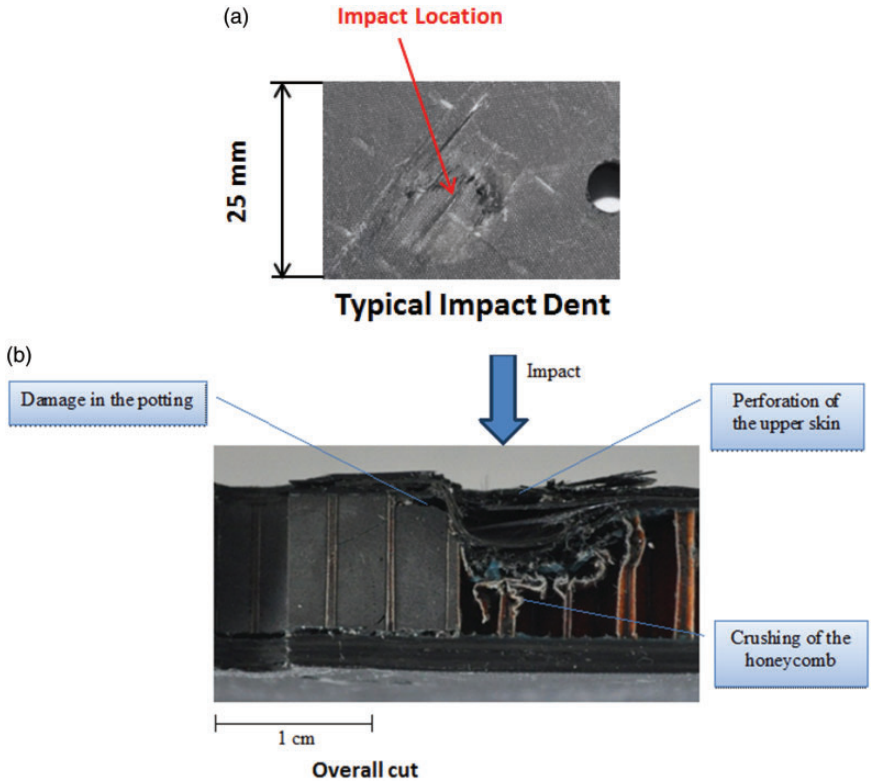

Figure 17. (a) Typical dent after impact and (b) post-mortem observation of a specimen impacted on the core.

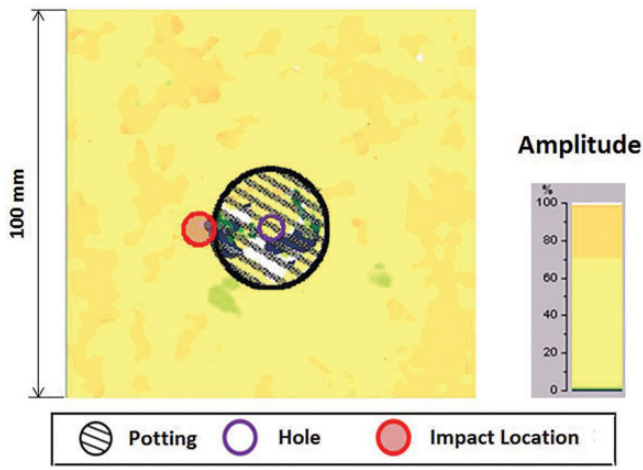

Figure 18. C-scan of the lower skin after an impact on the honeycomb core.

Table 1. Summary of damages occurring in the impact on a potted insert.

	Damages		
Impact location	Upper skin	Core	Lower skin
Potting	Slight indentation	Cracking 45° of the honeycomb, local crushing	Large delamination
Border	Indentation, slight punching	Cracking 45° of the honeycomb, crushing	Large delamination
Honeycomb	punching	Crushing of the honeycomb	No delamination

the impact occurs on the honeycomb. In this case, the skin is perforated locally and the honeycomb absorbs a large part of the energy. So the lower skin is protected and no damage is found.

Pull-through after impact tests

Test on pristine specimen

It was important to perform a test that would serve as a reference for explaining the failure scenarios and differences between the impact cases. The test curve is given in Figure 19. The curve is partially similar to Bunyawanichakul's results [18, 19]. Part 1 is the linear response without damage. Part 2 is limited by a first change in slope and a slight load jump followed by a recovery of stiffness. To check the damage mode in this phase, a test was stopped and a C-scan taken. It showed that the skins were not damaged (Figure 19). A section also showed no damage in the core, which is consistent with the scenario of post-buckling shear in cells of the honeycomb in the vicinity of the insert presented in the literature [18,19]. Damage in Zone 3 was not clearly identified as it was not possible to do a stopped test because of a lack of pristine specimens (only 2). The behaviour diverged from the literature [18,19]. An explanation will be given by analogy with test impacted specimens later. The shape of the plateau zone (4) clearly showed that the screw punched the lower skin.

Test on impacted specimens

The force/displacement curves for the four configurations are shown in Figure 20. The curves are very similar despite quite different damage patterns. If we look at higher loads, or Zone 4, it is clear that the reduction related to the impacts is weak, especially when compared to compression after impact tests [2, 8,9]. The know-down is less than 5% in case of impact on the insert and remains below 15% in case of impact on the edge or on the core. In the case of impact on the insert, the main type of damage is delamination in the lower skin. These delaminations have very

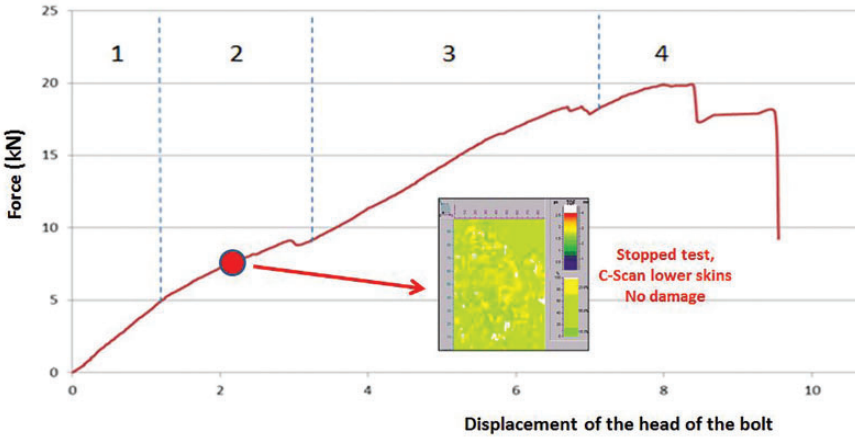

Figure 19. Pull-through test on a pristine specimen.

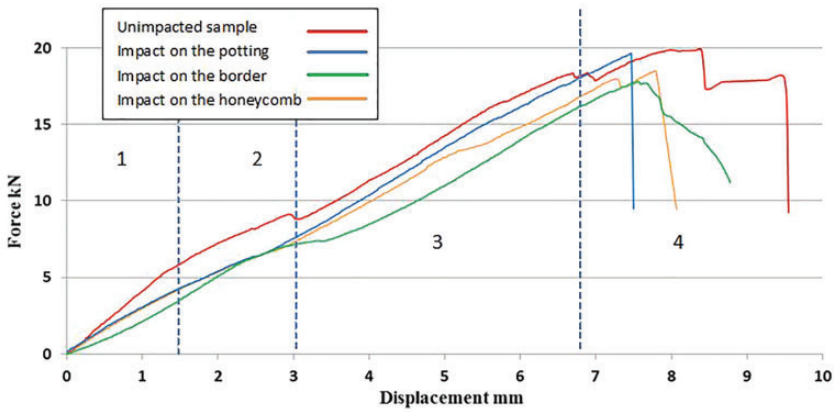

Figure 20. Comparison of pull-through response for the different cases.

little influence on the sandwich bending stiffness. The final failure is driven by the punching of the lower skin [17,18]. So the impact damage modes on the insert do not have any great influence on the final failure. In the case of impact on the core, the damaged upper skin area is limited and, in the same way, has little influence on the final rupture scenario even though the reduction is more significant here. However, in the case of the pristine sample, the maximum displacement at failure is greater and the punch most progressive. It is possible that the punching of the lower skin interacts with a local buckling of the lower skin occurring due to the large delamination and the compression caused by overall bending. The other possibility is that the upper side impact creates local splitting that generates a sharp break. A post-mortem pattern with such splitting is shown in Figure 21(b) and one of these local buckling events is shown in Figure 21(a).

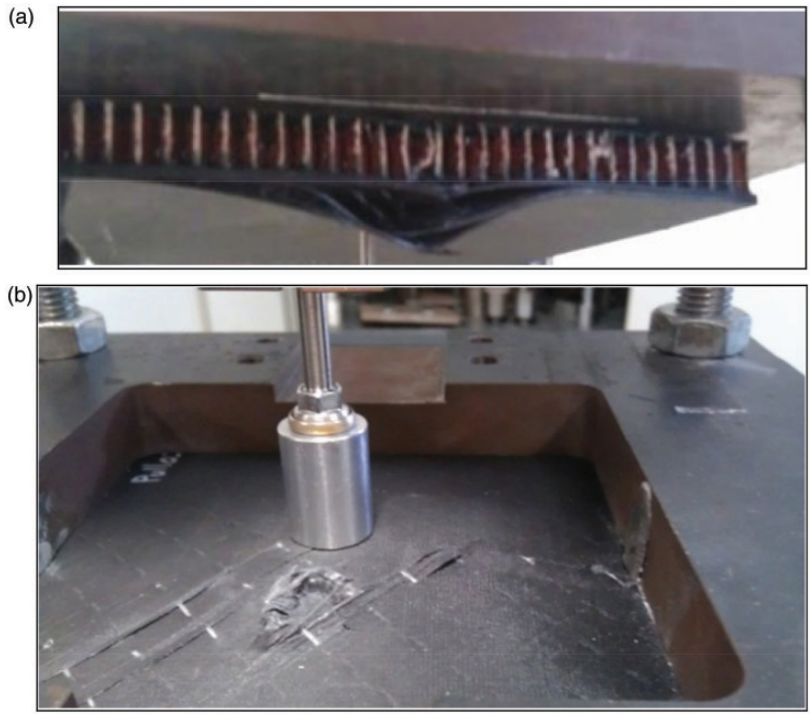

Figure 21. (a) Local buckling of the lower skin after pull-through, post-mortem view, case of impact on insert. (b) Failure pattern of the upper skin with splitting of the upper ply near the impact.

If we look at part 1 of the test curves, we see that the slope of the three damaged inserts is similar while the slope of the pristine sample is higher. Then in part 2, the slopes become identical. As the C-scan of the stopped test (Figure 19) did not show any delamination in the lower skin, the first damage of the pristine sample can be attributed to post-buckling of the cells of the honeycomb in the vicinity of the insert. This scenario has already been demonstrated by Bunyawanichakul et al. [17,18] both numerically and experimentally. Since the slope of the pristine sample is identical to those of the impacted specimens in part 2, it can be deduced that the honeycomb cells of these specimens are also sufficiently damaged during the impact to lose their initial stiffness. This observation is consistent with the qualitative observations of Figures 10, 14 and 17. The behaviour in zone 3 is more difficult to explain. The four types of specimens have the same slope, which would mean a priori that the damage is identical and that the slight jump up from the areas 2 and 3 of the pristine specimen corresponds to the creation of identical damage. Nevertheless, it has been shown that the damages of the three impacted specimens are quite differents. Only one stopped test was conducted in this area, on the specimen impacted on the honeycomb, and cracks were found near the drilled

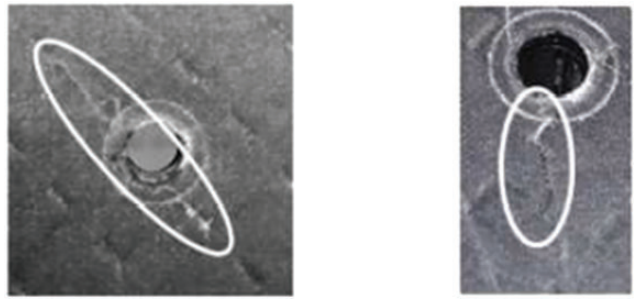

Figure 22. Local crack around the hole drilled in the lower skin, impact on the honeycomb core specimen.

hole in the lower skin (Figure 22). This shows that the damage occurring during the tests was probably more complex and coupled.

Conclusion

An experimental study was conducted on impacts on an insert in sandwich structures. The behaviour and damage varied according to the position of impact: on the insert, on the edge of the insert or on the core. In the first two cases, the insert transmitted the impact force to the lower skin of the sandwich, creating large delaminations in it. In the case of an impact on the core, classical damage was retrieved and the lower skin and the insert were little affected. Pull-through tests were carried out and, whatever the impact location, the strength after impact remained high, losses of only 5–15% being observed. The full damage scenario is difficult to identify because many modes interact: buckling and fracture of the honeycomb cells, punch of the skin, delaminations, local buckling, fibre breakage near the hole edge. Only a dialogue between testing and calculation and more stopped tests would clarify the failure scenario. The modelling is challenging and only very advanced models, e.g. the discrete ply model used by the authors on similar problems [29, 32], would capture damage in the skin. A fully nonlinear model able to capture compression/shear buckling of Nomex honeycomb, like the one recently developed by Seemann and Krause [33], is also necessary.

Declaration of Conflicting Interests

The author(s) declared no potential conflicts of interest with respect to the research, authorship, and/or publication of this article.

Funding

The author(s) disclosed receipt of the following financial support for the research, authorship, and/or publication of this article: The authors wish to thank Sogeclair Aerospace for their financial and operational support.

References

1. Castanié B, Bouvet C, Aminanda Y, et al. Modelling of low energy/low velocity impact on nomex honeycomb sandwich structures with metallic skins. *Int J Imp Eng* 2008; 35: 620–634.
2. Castanié B, Aminanda Y, Bouvet C, et al. Core crush criteria to determine the strength of sandwich composite structures subjected to compression after impact. *Comp Struct* 2008; 86: 243–250.
3. Hayman B. Approaches to damage assessment and damage tolerance for FRP sandwich structures. *J Sand Struct Mater* 2007; 9: 571–595.
4. Raju KS, Smith BL, Tomblin JS, et al. Impact damage resistance and tolerance of honeycomb core sandwich panels. *J Compos Mater* 2008; 42: 385–412.
5. Anderson T and Madenci E. Experimental investigation of low-velocity impact characteristics of sandwich composites. *Compos Struct* 2000; 50: 239–247.
6. Zenkert D, Shipsha A, Bull P, et al. Damage tolerance assessment of composite sandwich panels with localised damage. *Compos Sci Technol* 2005; 65: 2597–2611.
7. McQuigg TD. *Compression after impact experiments and analysis on honeycomb core sandwich panels with thin facesheets*. NASA/CR–2011-217157, National Institute of Aerospace, Hampton, Virginia, USA, 2011.
8. Abrate S. *Impact on composite structures*. New York, USA: Cambridge University Press, 1998.
9. Abrate S, Castanié B and Rajapakse YDS. *Dynamic failure of composite and sandwich structures*. Dordrecht, The Netherlands: Springer, 2012.
10. ZenKert D. *Sandwich construction*. Cradley Heath, UK: EMAS Publishing, 1997.
11. US Military Handbook 23A. *Design of flat circular sandwich panels loaded at an insert*, 1974..
12. Insert design handbook, ESA PSS 03–1202, Noordwijk, The Netherlands: European Space Research and Technology Centre, 1987.
13. Thomsen OT. Sandwich plates with 'through-the-thickness' and 'fully-potted' insert: evolution of differences in structural performance. *Compos Struct* 1998; 40: 159–174.
14. Thomsen OT and Ritz W. Analysis and design of sandwich plates with inserts – a high-order sandwich plate theory approach. *Compos B* 1998; 29: 795–807.
15. Bozhevolnaya E, Thomsen OT, Kildegaard A, et al. Local effects across core junctions in sandwich panels. *Compos B* 2003; 34: 509–517.
16. Bozhevolnaya E and Lyckegaard A. Structurally graded core inserts in sandwich panels. *Compos Struct* 2005; 9: 68–23.
17. Bunyawanichakul P, Castanié B and Barrau JJ. Experimental and numerical analysis of inserts in sandwich structures. *Appl Compos Mater* 2005; 12: 177–191.
18. Bunyawanichakul P, Castanié B and Barrau JJ. Nonlinear finite element analysis of inserts in sandwich structures. *Compos B* 2008; 39: 1077–1092.
19. Raghu N and Battley MT. Southward. Strength variability of inserts in sandwich panels. *J Sand Struct Mater* 2009; 11: 501–517.
20. Smith B and Banerjee B. Reliability of inserts in sandwich composite panels. *Compos Struct* 2012; 94: 820–829.
21. Jun Woo L and Lee DG. Development of the hybrid insert for composite sandwich satellite structures. *Compos A* 2011; 42: 1040–1048.
22. New Insert allows automatic placement in composite sandwich panels, JEC Magazine 2015, May–June, p27.

23. Yong Bin P, Hwe Kweon J and Ho Choi J. Failure characteristics of carbon/BMI-Nomex sandwich joints in various hygrothermal conditions. *Compos B* 2014; 60: 213–221.
24. Heimbs S and Pein M. Failure Behaviour of honeycomb sandwich corner joints and inserts. *Compos Struct* 2009; 89: 575–588.
25. Roy R, Nguyen KH, Park YB, et al. Testing and modeling of nomex TM honeycomb sandwich panels with bolt insert. *Compos B* 2013; 56: 762–769.
26. Song KI, Choi JY, Kweon JH, et al. An experimental study of the insert joint strength of composite sandwich structures. *Compos Struct* 2008; 86: 107–113.
27. Dols S, Bouvet C, Castanié B, et al. Post-impact behavior of insert in sandwich structures. In: *Proceedings of 11th international conference on sandwich structures ICSS-11*, Fort Lauderdale, 21–22 March 2016..
28. Dols S, Bouvet C, Castanié B, et al. Impact et tenue résiduelle des inserts de structures sandwichs. In: *Proceedings of JNC 18, Journées Nationales sur les composites,* Nantes, 12–14 June 2013..
29. Adam L, Bouvet C, Castanié B, et al. Discrete ply model of circular pull-through test of fasteners in laminates. *Compos Struct* 2012; 94: 3082–3091.
30. Hongkarnjanakul N, Bouvet C and Rivallant S. Validation of low velocity impact modelling on different stacking sequences of CFRP laminates and influence of fibre failure. *Compos Struct* 2013; 106: 549–559.
31. Aminanda Y, Castanié B, Barrau JJ, et al. Experimental analysis and modeling of the crushing of honeycomb cores. *Appl Compos Mater* 2005; 12: 213–217.
32. Achard V, Bouvet C, Castanié B, et al. Discrete ply modelling of open hole tensile tests. *Compos Struct* 2014; 113: 369–381.
33. Seemann R and Krause D. Numerical modeling of nomex honeycomb sandwich cores at meso-scale level. *Compos Struct* 2017; 159: 702–718.